BER of Noncoherent MFSK with Postdetection Switch-and-Stay Combining in TWDP Fading

Sasan Haghani, *Member, IEEE* and Hadis Dashtestani, *Student Member, IEEE*

Department of Electrical and Computer Engineering, University of the District of Columbia, Washington DC, 20008
E-mail: {shaghani,hadis.dashtestani}@udc.edu

***Abstract*—The performance of noncoherent M-ary frequency-shift keying (MFSK) with dual-branch postdetection switch and stay combining (SSC) in two-wave with diffuse power (TWDP) fading is studied. A closed-form expression for the average bit error rate (BER) of noncoherent MFSK with dual-branch postdetection SSC is derived. Monte carlo simulation results are presented to verify the validity of the obtained analytical expressions. The effects of TWDP fading parameters on the relative performances of postdetection and predetection SSC receivers are studied. It is shown that postdetection SSC has superior performance over predetection SSC.**

***Index Terms*—Diversity combining, fading channels, noncoherent frequency shift keying, predetection diversity, postdetection diversity, Rayleigh fading, Rician fading, two-wave with diffuse power fading.**

I. Introduction

DIVERSITY is an effective technique to combat fading in wireless communication systems. Switch-and-Stay combining (SSC) is one of the simplest diversity techniques where the receiver selects a particular branch as long as its quality is above a predetermined threshold. If the quality of the selected branch falls below the predetermined threshold, the receiver switches to the other branch regardless of the quality of that branch [1]. SSC systems have been suggested for low complexity receivers where the number of diversity branches are equal to two [1]. Inexpensive receiver chips that output the demodulated signal are available for some applications, motivating a study of postdetection diversity schemes.

Two types of SSC receivers are studied in the literature; postdetection SSC and predetection SSC. In predetection SSC, the switching of the receiver is based on the instantaneous signal-to-noise ratios (SNRs) on the diversity branches. However, in postdetection SSC, the switching strategy is based on the receiver statistics that are used for data detection [1]. Two types of postdetection SSC are considered in the literature. In this paper, we refer to these receiver structures as postdetection SSC Model 1 and Model 2. Postdetection SSC Model 1 was proposed in [1] and can be used with binary frequency shift-keying (BFSK) only, whereas the postdetection SSC Model 2 receiver introduced in [2] is designed to operate using noncoherent M-ary frequency shift-keying (MFSK).

In wireless communication systems, the Rayleigh and Rician distributions are often used to characterize the envelope of the received signal. In scenarios where there is no line-of-sight (LOS) between the transmitter and the receiver the Rayleigh distribution is used whereas in cases when there is a strong LOS between the transmitter and the receiver, the Rician distribution is used. There are however scenarios that the envelope of the received signal contains two strong multipath waves in addition to the diffuse components [3]. This could occur when directional antennas and wide-band signals are used at the receiver. Directional antennas or arrays at the receiver can amplify several of the strongest multipath waves resulting in two-wave with diffuse power (TWDP) fading [3]. Recently, it has also been observed that TWDP fading can better model small scale fading in wireless sensor networks [4]. Rayleigh and Rician fading are special cases of the TWDP fading.

The performance of noncoherent BFSK and MFSK with dual-branch SSC in Rayleigh and Rician fading has been well studied in the literature, both for independent and correlated fading channels [5]-[8]. While analytical results exist for the performance of noncoherent BFSK with predetection and postdetection Model 1 in TWDP fading [9], [10], no analytical results are available for the performance of MFSK with postdetection SSC Model 2 in TWDP fading. In this paper, we obtain analytical expressions for the average bit error rate (BER) of MFSK with postdetection SSC Model 2 in TWDP fading. We assume that the fadings on the diversity branches are independent but not necessarily identically distributed. Analytical expressions for the performance of noncoherent MFSK with predetection SSC are also given which enable us to compare the performances of the predetection and postdetection receivers.

The remainder of this paper is organized as follows. In Section II, a brief overview of TWDP fading is given. The average BERs of noncoherent MFSK with postdetection SSC Model 2 and predetection SSC are analyzed in Sections III and IV, respectively. Numerical examples are given in Section V where the performances of postdetection SSC Model 1 and Model 2 are compared to the performance of predetection SSC. Finally, some conclusions are given in Section VI.

II. Two-Wave with Diffuse Power Fading

Two-wave with diffuse power fading was recently proposed in [3] to model a communications channel where there are two specular multipath components in the presence of diffusely propagating waves. While a closed-form expression for the probability density function (PDF) of TWDP fading does not

978-1-4673-1881-5/12/$31.00 ©2012 IEEE

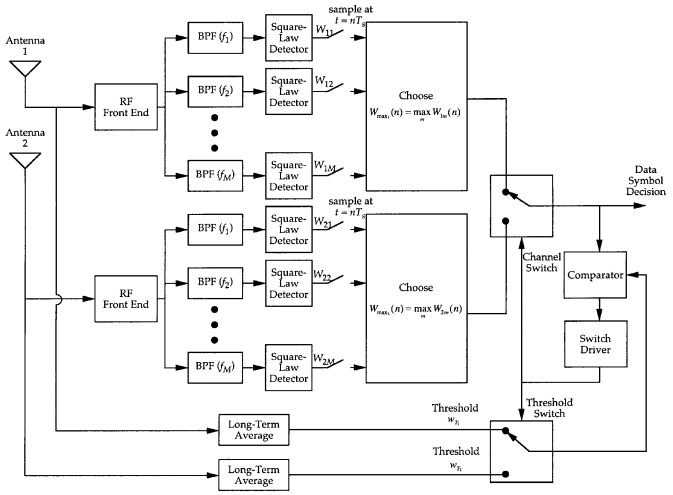

Fig. 1. The block diagram of the noncoherent MFSK receiver with postdetection SSC (after [2, Fig.]).

exist, a closed-form expression was developed in [3] that closely approximates the behavior of the exact PDF and is given by

$$f_\alpha(x) = \frac{x}{\sigma^2}\exp\left(-\frac{x^2}{2\sigma^2} - K\right) \times \sum_{l=1}^{L} a_l D\left(\frac{x}{\sigma}, K, \Delta\cos\frac{\pi(l-1)}{2L-1}\right) \tag{1a}$$

where

$$D(x,K,y) = \frac{1}{2}\exp(yK)I_0\left(x\sqrt{2K(1-y)}\right) + \frac{1}{2}\exp(-yK)I_0\left(x\sqrt{2K(1+y)}\right) \tag{1b}$$

and

$$a_l = \frac{2(-1)^l}{(2L-1)(2L-l)!(l-1)!} \times \int_0^{2L-1}\prod_{k=1,k\neq l}^{2L}(u-k+1)du. \tag{1c}$$

In (1), $K = \frac{V_1^2+V_2^2}{2\sigma^2}$ and $\Delta = \frac{2V_1V_2}{V_1^2+V_2^2}$, where V_1 and V_2 are the voltage magnitudes of the two specular waves and $2\sigma^2$ is the average power of the diffuse waves. The parameters K and Δ represent the ratio of the average specular power to the average diffuse power and the relative strength of the two specular components, respectively. Also, in (1), L is the order of the approximate TWDP PDF and is selected such that $L > \frac{1}{2}K\Delta$ so that (1) accurately models the exact pdf [3]. The values of $a_i, i = 1,\cdots,5$ are given in [3, Table 2]. Note that the TWDP PDF given in (1) reduces to the *exact* Rician PDF for $\Delta = 0$ and to the *exact* Rayleigh PDF for $K = 0$.

III. Average BER Analysis of Postdetection SSC

A block diagram of the dual-branch postdetection SSC Model 2 system employing noncoherent MFSK is given in Fig. 1. Let $W_{im}(n), i = 1,2, m = 1,\cdots,M$ denote the outputs of the M square law detectors of the receiver at the sampling instant $t = nT_s$, where T_s is the symbol sampling interval and where the subscript i in W_{im} denotes the diversity branch. Assuming that the symbol corresponding to the first message in the alphabet is transmitted, W_{im} can be written as [2]

$$W_{i1}(n) = |2E_s\alpha_i e^{j\theta_i} + N_{i1}|^2 \tag{2}$$

$$W_{im}(n) = |N_{im}|^2, i = 1,2, m = 2,3,\cdots,M \tag{3}$$

where $j = \sqrt{-1}$, E_s is the transmitted energy per symbol, $\alpha_i e^{j\theta_i}, i = 1,2$ are the complex channel gains on channels 1, 2 and N_{ij} are zero-mean complex Gaussian random variables (RVs) with variance $4E_sN_0$. The switching mechanism is based on the comparison of the maximum of the square-law detector outputs on each branch with a predetermined threshold w_{T_i}. As an example, if the switch is connected to Antenna 1, it will stay connected to Antenna 1 as long as $W_{\max_1}(n) \triangleq \max W_{1m}(n) > w_{T_1}$. If $W_{\max_1}(n) < w_{T_1}$ the system will switch to Antenna 2 regardless of whether $W_{\max_2}(n) \triangleq \max W_{2m}(n)$ is greater or less than the predetermined threshold w_{T_2}.

Assume that the switch is connected to Antenna 1. Then, following the analysis in [2], the probability of a correct decision can be written as

$$\begin{aligned} P_{s1}(C) = \Pr[&W_{11}(n) \geq w_{T_1}, W_{12}(n) < W_{11}(n), \\ &W_{13}(n) < W_{11}(n),\cdots,W_{1M}(n) < W_{11}(n)] \\ &+ \Pr[W_{\max_1}(n) \leq w_{T_1}, W_{22}(n) < W_{21}(n), \\ &W_{23}(n) < W_{21}(n),\cdots,W_{2M}(n) < W_{21}(n)]. \end{aligned} \tag{4}$$

Noting that $W_{1m}, m = 1,\cdots,M$ are independent and $W_{1m}, m = 2,\cdots,M$ are independent and identically distributed (i.i.d), $P_{s1}(C)$ can be written as [2, eq. (3)]

$$P_{s1}(C) = \int_{w_{T_1}}^{\infty} f_{W_{11}}(x)[F_{W_{12}}(x)]^{M-1}dx + F_{W_{11}}(w_{T_1}) \times [F_{W_{12}}(w_{T_1})]^{M-1}\int_0^{\infty} f_{W_{21}}(x)[F_{W_{22}}(x)]^{M-1}dx \tag{5}$$

where $f_{W_{im}}(\cdot)$ and $F_{W_{im}}(\cdot)$ denote the PDF and the cumulative distribution function (CDF) of the RV W_{im}, respectively. Similarly, the probability of a correct decision when the switch is connected to Antenna 2, denoted as $P_{s2}(C)$, can be computed as [2, eq. (4)]

$$P_{s2}(C) = \int_{w_{T_2}}^{\infty} f_{W_{21}}(x)[F_{W_{22}}(x)]^{M-1}dx + F_{W_{21}}(w_{T_2}) \times [F_{W_{22}}(w_{T_2})]^{M-1}\int_0^{\infty} f_{W_{11}}(x)[F_{W_{12}}(x)]^{M-1}dx. \tag{6}$$

Let p_i denote the percentage of time that the switch is connected to Antenna i. Then, using a two-state Marcov chain process, it is shown in [2] that p_1 and p_2 can be computed as

$$p_1 = \frac{F_{W_{21}}(w_{T_2})[F_{W_{22}}(w_{T_2})]^{M-1}}{\sum_{i=1}^{2} F_{W_{i1}}(w_{T_i})[F_{W_{i2}}(w_{T_i})]^{M-1}} \tag{7}$$

$$p_2 = \frac{F_{W_{11}}(w_{T_1})[F_{W_{12}}(w_{T_1})]^{M-1}}{\sum_{i=1}^{2} F_{W_{i1}}(w_{T_i})[F_{W_{i2}}(w_{T_i})]^{M-1}}. \tag{8}$$

The probability of correct decision can now be obtained as $P_s(C) = p_1 P_{s1}(C) + p_2 P_{s2}(C)$. Thus, the average symbol error rate (SER) can be computed as $P_s(E) = 1 - P_s(C)$. Note that the average BER can be obtained from the average SER using [11]

$$\begin{aligned} P_b(E) &= \frac{M}{2(M-1)} P_s(E) \\ &= \frac{M}{2(M-1)} \left(1 - p_1 P_{s1}(C) - p_2 P_{s2}(C)\right). \end{aligned} \tag{9}$$

To proceed, we start by calculating the CDF of W_{i1}. Assuming the channel is static, one can see that W_{i1} is a non-central chi-squared RV with two degrees of freedom and its CDF is given by [11]

$$F_{W_{i1}|\alpha_i}(x) = 1 - Q_1\left(\sqrt{2\gamma_i}, \sqrt{\frac{x}{2E_s N_0}}\right) \tag{10}$$

where $\gamma_i = \dfrac{E_s \alpha_i^2}{N_0}$ is the instantaneous SNR on the ith branch and $Q_1(a,b)$ is the first order Marcum Q-function [12, eq. (4.11)]. Let $\bar{\gamma_i} = E(\gamma_i)$, where $E(\cdot)$ denotes expectation. Then, it can be shown that $\bar{\gamma_i}$ is given by

$$\bar{\gamma_i} = \frac{2\sigma_i^2 (1+K_i) E_s}{N_0} \tag{11}$$

where σ_i^2 and K_i are the fading parameters associated with the ith branch. Averaging $F_{W_{i1}|\alpha_i}(x)$ over the PDF of α_i, as given in (1), and using (11) and [13, eqn. B.31], the unconditional CDF of W_{i1} is obtained as

$$\begin{aligned} F_{W_{i1}}(x) &= 1 - \frac{1}{2}\sum_{l=1}^{L_i} a_l \\ &\times \left[Q_1\left(\sqrt{\frac{2K_i\bar{\gamma_i}(1-\lambda_i(l))}{\bar{\gamma_i}+1+K_i}}, \sqrt{\frac{(1+K_i)x}{2E_sN_0(\bar{\gamma_i}+1+K_i)}}\right) \right. \\ &\left. + Q_1\left(\sqrt{\frac{2K_i\bar{\gamma_i}(1+\lambda_i(l))}{\bar{\gamma_i}+1+K_i}}, \sqrt{\frac{(1+K_i)x}{2E_sN_0(\bar{\gamma_i}+1+K_i)}}\right) \right] \end{aligned} \tag{12}$$

where K_i and Δ_i are the TWDP parameters on the ith channel, L_i is the order of the approximate PDF on the ith branch and $\lambda_i(l) = \Delta_i \cos\left(\dfrac{\pi(l-1)}{2L_i - 1}\right)$. The PDF of W_{i1} can now be calculated from its CDF as

$$\begin{aligned} f_{W_{i1}}(x) &= \frac{1+K_i}{8E_sN_0(1+K_i+\bar{\gamma_i})} \exp\left(-\frac{(1+K_i)x}{\bar{\gamma_i}+K_i+1}\right) \\ &\times \sum_{l=1}^{L_i} a_l \left[\exp\left(-\frac{K_i\bar{\gamma_i}(1-\lambda_i(l))}{1+K_i+\bar{\gamma_i}}\right) \right. \\ &\times I_0\left(\sqrt{\frac{K_i\bar{\gamma_i}(1+K_i)(1-\lambda_i(l))x}{E_sN_0(1+K_i+\bar{\gamma_i})^2}}\right) \\ &+ \exp\left(-\frac{K_i\bar{\gamma_i}(1+\lambda_i(l))}{1+K_i+\bar{\gamma_i}}\right) \\ &\left. \times I_0\left(\sqrt{\frac{K_i\bar{\gamma_i}(1+K_i)(1+\lambda_i(l))x}{E_sN_0(1+K_i+\bar{\gamma_i})^2}}\right) \right]. \end{aligned} \tag{13}$$

Next, we can see that $W_{im}, i = 1, 2, m = 2, 3, \cdots, M$ are central chi-squared RVs with two degrees of freedom. Hence, their PDFs and CDFs are given by

$$f_{W_{im}}(x) = \frac{1}{4E_sN_0} \exp\left(-\frac{x}{4E_sN_0}\right) \tag{14}$$

and

$$F_{W_{im}}(x) = 1 - \exp\left(-\frac{x}{4E_sN_0}\right), \tag{15}$$

respectively. Substituting (12), (13), (14) and (15) in (5), using [13, eqns. B.22 and B.23], and after much mathematical manipulations and simplifications $P_{s1}(C)$ is calculated as (16) shown at the bottom of the page where $g_i(p) = (K_i+1)(1+p) + p\bar{\gamma_i}$, $\Omega_i = E(\alpha_i^2)$ and where $\eta_{T_i} = \frac{w_{T_i}}{E_s^2\Omega_i}$ is the normalized switching threshold. A similar expression can be obtained for $P_{s2}(C)$ and is omitted here for the sake of brevity. The average BER of noncoherent MFSK with postdetection SSC Model 2 can now be calculated by substitution of the expressions

---

$$\begin{aligned} P_{s1}(C) &= \sum_{l=1}^{L_1} a_l \left[\sum_{p=0}^{M-1} \binom{M-1}{p} (-1)^p \left(\frac{1+K_1}{g_1(p)}\right) \times \right. \\ &\left\{ \frac{1}{2}\exp\left(-\frac{K_1 p\bar{\gamma_1}(1-\lambda_1(l))}{g_1(p)}\right) \times Q_1\left(\sqrt{\frac{2K_1\bar{\gamma_1}(1+K_1)(1-\lambda_1(l))}{g_1(p)(1+K_1+\bar{\gamma_1})}}, \sqrt{\frac{\bar{\gamma_1}\eta_{T_1}g_1(p)}{2(1+K_1+\bar{\gamma_1})}}\right) + \right. \\ &\left. \left. \frac{1}{2}\exp\left(-\frac{K_1 p\bar{\gamma_1}(1+\lambda_1(l))}{g_1(p)}\right) \times Q_1\left(\sqrt{\frac{2K_1\bar{\gamma_1}(1+K_1)(1+\lambda_1(l))}{g_1(p)(1+K_1+\bar{\gamma_1})}}, \sqrt{\frac{\bar{\gamma_1}\eta_{T_1}g_1(p)}{2(1+K_1+\bar{\gamma_1})}}\right) \right\} \right] + \left[1 - \frac{1}{2} \right. \\ &\left. \times \sum_{l=1}^{L_1} a_l \left\{ Q_1\left(\sqrt{\frac{2K_1\bar{\gamma_1}(1-\lambda_1(l))}{1+K_1+\bar{\gamma_1}}}, \sqrt{\frac{(1+K_1)\bar{\gamma_1}\eta_{T_1}}{2(1+\bar{\gamma_1}+K_1)}}\right) + Q_1\left(\sqrt{\frac{2K_1\bar{\gamma_1}(1+\lambda_1(l))}{1+K_1+\bar{\gamma_1}}}, \sqrt{\frac{(1+K_1)\bar{\gamma_1}\eta_{T_1}}{2(1+\bar{\gamma_1}+K_1)}}\right) \right\} \right] \times \\ &\left(1 - \exp\left(-\frac{\bar{\gamma_1}\eta_{T_1}}{4}\right)\right)^{M-1} \times \sum_{l=1}^{L_2} a_l \left\{ \sum_{p=0}^{M-1} \binom{M-1}{p} (-1)^p \left(\frac{1+K_2}{g_2(p)}\right) \right. \\ &\left. \times \left[\frac{1}{2}\exp\left(-\frac{K_2 p\bar{\gamma_2}(1-\lambda_2(l))}{g_2(p)}\right) + \frac{1}{2}\exp\left(-\frac{K_2 p\bar{\gamma_2}(1+\lambda_2(l))}{g_2(p)}\right) \right] \right\}. \end{aligned} \tag{16}$$

$P_{s1}(C)$ and $P_{s2}(C)$ in (9). Note that p_1 and p_2 can be easily calculated using the CDFs of the RVs $W_{i1}, i = 1, 2$ and W_{22}, which are given in eqs. (12) and (15), respectively. For example, if the channels are i.i.d, $p_1 = p_2 = \frac{1}{2}$, and the average BER becomes $P_b(E) = \frac{M}{2(M-1)}(1 - P_{s1}(C))$.

The optimum switching threshold, η_T^*, that minimizes the average BER can now be obtained by solving

$$\left.\frac{dP_b(E)}{d\eta_T}\right|_{\eta_T=\eta_T^*} = 0. \tag{17}$$

IV. Average BER Analysis of Predetection SSC

In this section we provide an analytical expression for the average BER of noncoherent MFSK in predetection SSC. We assume that the fading on the branches are independent and have the same average fading power, i.e., $\bar{\gamma} = \bar{\gamma_1} = \bar{\gamma_2}$, and the same fading parameters $\Delta = \Delta_1 = \Delta_2$ and $K = K_1 = K_2$. The average BER of noncoherent BFSK with predetection SSC was computed in [10]. For noncoherent MFSK, using similar steps to that of [10, Section IV], we obtain the average SER of MFSK with predetection SSC as

$$\begin{aligned}
P_s(E) = &\sum_{i=1}^{M-1} \frac{(1+K)(-1)^{i+1}\binom{M-1}{i}}{2(i+1)(1+K+\bar{\gamma}\beta(i))} \Bigg(F_\gamma(\eta_T) \sum_{l=1}^{L} a_l \Bigg\{ \\
&\exp\left(-\frac{K(1-\lambda(l))\bar{\gamma}\beta(i)}{1+K+\bar{\gamma}\beta(i)}\right) + \exp\left(-\frac{K(1+\lambda(l))\bar{\gamma}\beta(i)}{1+K+\bar{\gamma}\beta(i)}\right) \Bigg\} \\
&+ \sum_{l=1}^{L} a_l \Bigg[\exp\left(-\frac{K(1-\lambda(l))\bar{\gamma}\beta(i)}{1+K+\bar{\gamma}\beta(i)}\right) \\
&\times Q_1\left(\sqrt{\frac{2K(1+K)(1-\lambda(l))}{1+K+\bar{\gamma}\beta(i)}}, \sqrt{\frac{(1+K+\bar{\gamma}\beta(i))\eta_T}{\bar{\gamma}}}\right) \\
&+ \exp\left(-\frac{K(1+\lambda(l))\bar{\gamma}\beta(i)}{1+K+\bar{\gamma}\beta(i)}\right) \\
&\times Q_1\left(\sqrt{\frac{2K(1+K)(1+\lambda(l))}{1+K+\bar{\gamma}\beta(i)}}, \sqrt{\frac{(1+K+\bar{\gamma}\beta(i))\eta_T}{\bar{\gamma}}}\right) \Bigg] \Bigg)
\end{aligned} \tag{18}$$

where $\lambda(l) = \Delta\cos\left(\frac{\pi(l-1)}{2L-1}\right)$, $\beta(i) = \frac{i}{i+1}$, η_T denotes the switching threshold and

$$\begin{aligned}
F_\gamma(x) = 1 - \frac{1}{2}\sum_{l=1}^{L} a_l \Bigg\{ &Q_1\left(\sqrt{2K(1-\lambda(l))}, \sqrt{\frac{2(1+K)x}{\bar{\gamma}}}\right) \\
&+ Q_1\left(\sqrt{2K(1+\lambda(l))}, \sqrt{\frac{2(1+K)x}{\bar{\gamma}}}\right) \Bigg\}.
\end{aligned} \tag{19}$$

The average BER can now be calculated from the average SER using $P_b(E) = \frac{M}{2(M-1)}P_s(E)$. Note that for $M = 2$, corresponding to BFSK, (18) reduces to [10, eq. (26)], as expected. The optimum switching threshold can now be computed by using (17).

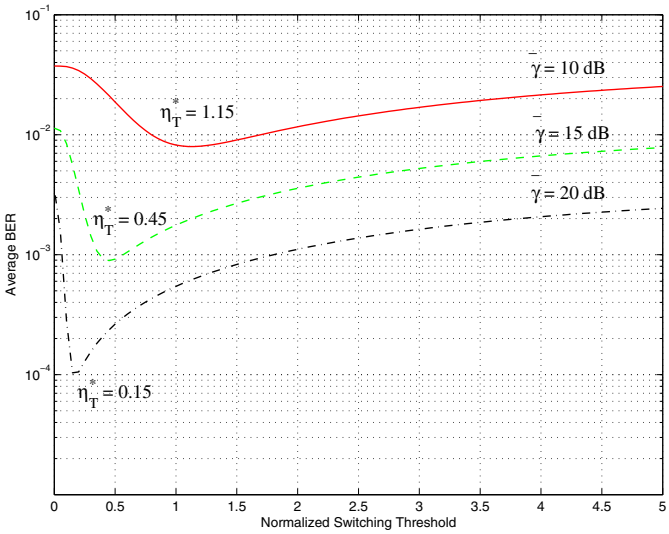

Fig. 2. The average BER of QFSK with postdetection SSC as a function of the switching threshold for $K = 3$ dB, $\Delta = 0.6$ and $\bar{\gamma} = 10, 15$ and 20dB.

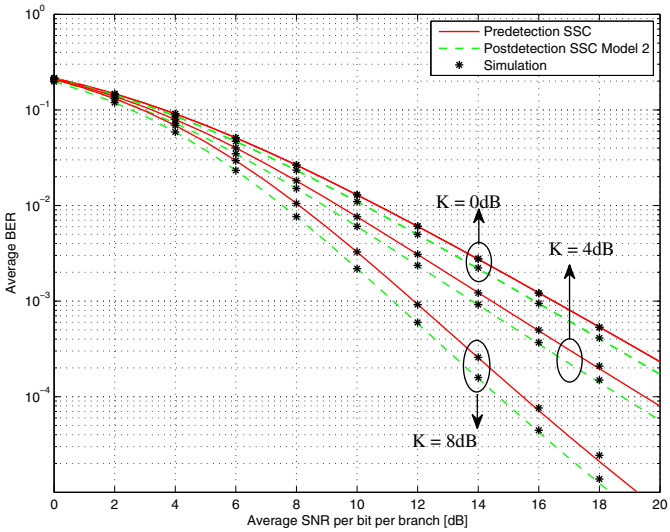

Fig. 3. The average BER of noncoherent QFSK with postdetection SSC Model 2 and predetection as a function of average SNR per bit per branch for $K = 0, 4$, and 8 and $\Delta = 0.5$.

V. Numerical Examples and Discussion

In this section, some numerical examples are presented to compare the performances of postdetection SSC receivers with that of predetection SSC. For postdetection SSC Model 1, we have used the analytical results developed in [10] to compute the BER values. Monte Carlo simulation results are also presented to test the validity of the analytical results obtained in Sections III and IV. We assume that the branches are i.i.d with $\bar{\gamma} = \bar{\gamma_1} = \bar{\gamma_2}$, $\Delta = \Delta_1 = \Delta_2$ and $K = K_1 = K_2$.

Fig. 2 shows the average BER of noncoherent quaternary frequency shift keying (QFSK) as a function of the normalized switching threshold in i.i.d TWDP fading with $\Delta = 0.6$ and $K = 3$ dB for $\bar{\gamma} = 10, 15$ and 20 dB. Fig. 2 indicates that the optimum switching threshold decreases as the average SNR increases, indicating that the system switches more often to take advantage of the channel conditions.

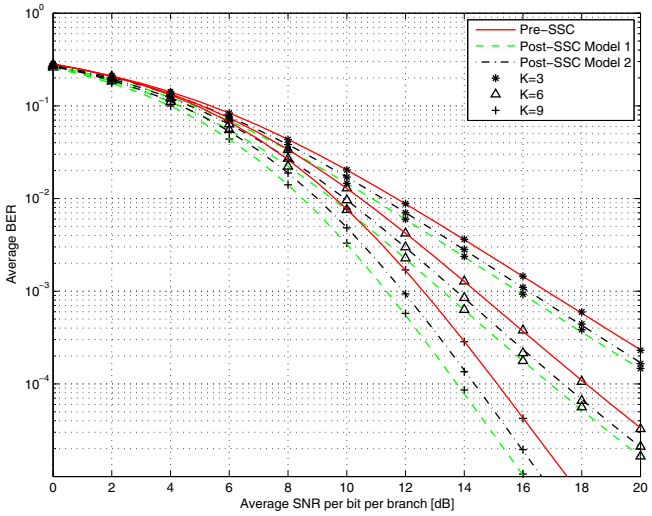

Fig. 4. The average BER of BFSK with postdetection SSC Model 1 and Model 2 and predetection SSC as a function of the average SNR per bit per branch for $K = 3, 6$ and 9 dB with $\Delta = 0.5$.

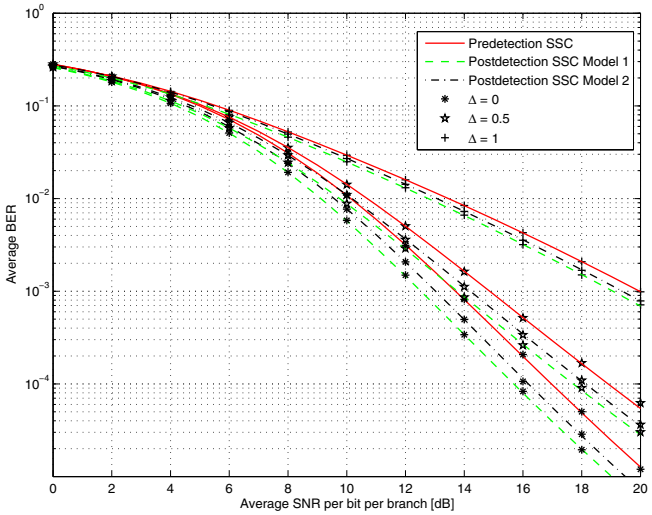

Fig. 5. The average BER of BFSK with postdetection SSC Model 1 and Model 2 and predetection SSC as a function of the average SNR per bit per branch for $K = 5$ dB and $\Delta = 0, 0.5$ and 1.

The average BER of noncoherent QFSK with postdetection SSC Model 2 and predetection SSC in TWDP fading is plotted in Fig. 3 for $\Delta = 0.5$ and $K = 0, 4$ and 8 dB. For each SNR value the optimum switching threshold is used for calculating the average BER. Fig. 3 shows that postdetection SSC Model 2 outperforms predetection SSC and the performance gap increases as the channels become less faded (corresponding to increasing K). For example, at an average BER of 10^{-3}, the SNR gap between postdetection SSC Model 2 and predetection SSC is 0.38, 0.60 and 0.70 for $K = 0, 4$ and 8 dB.

Fig. 4 shows the average BER of noncoherent BFSK with predetection and postdetection SSC Model 1 and Model 2 as a function of average SNR in i.i.d TWDP fading with $\Delta = 0.5$ and $K = 3, 6$ and 9 dB. For each average SNR value in Fig. 2, and for each receiver, the optimum switching threshold is used to plot the average BER. Fig. 4 shows that as the channel becomes less faded (larger K), the performance gap between predetection and postdetection SSC increases slightly. For example, at an average BER of 10^{-3}, the performance gap between predetection and postdetection SSC Model 1 is 0.98, 1.13 and 1.25dB for $K = 3, 6$ and 9 dB, respectively.

Finally, in Fig. 5, the impact of the fading parameter Δ on the performances of predetection and postdetection SSC receivers is studied where the average BER of noncoherent BFSK is plotted as a function of the average SNR per bit per branch for $K = 5$ dB and $\Delta = 0$, 0.5 and 1. Note that $\Delta = 0$ corresponds to Rician fading while $\Delta = 1$ corresponds to Hyper-Rayleigh fading [4]. Fig. 5, shows that as the channel becomes more faded (increasing Δ), the performance gap between the two postdetection SSC receivers and predetection SSC decreases. For example, at an average BER of 10^{-3} this difference is 1.20, 1.10 and 0.90 dB between Postdetection SSC Model 1 and predetection SSC for $\Delta = 0, 0.5$ and 1, respectively.

VI. Conclusion

In this paper, the performances of noncoherent MFSK with dual-branch predetection and postdetection SSC in TWDP fading were studied. Analytical results were obtained for the average BER of noncoherent MFSK with postdetection SSC in TWDP fading where the fadings where assumed to be independent but not identically distributed. The effects of channel fading parameters on the relative performances of postdetection SSC and predetection SSC receivers were analyzed and it was shown that postdetection SSC outperforms predetection SSC.

References

[1] M.-S. Alouini and M. K. Simon, "Postdetection Switched Combining-A Simple Diversity Scheme With Improved BER Performance," *IEEE Trans. Commun.*, vol. 51, pp. 1591–1602, Sept. 2003.

[2] M. K. Simon and M.-S. Alouini, "Probability of Error for noncoherent M-ary orthogonal FSK With Post-detection Switched Combining," *IEEE Trans. Commun.*, vol. 51, pp. 1456–1462, Sept. 2003.

[3] G. D. Durgin, T. S. Rappaport, and D. A. de Wolf, "New Analytical Models and Probability Density Functions for Fading in Wireless Communications," *IEEE Trans. Commun.*, vol. 50, pp. 1005–1015, Jun. 2002.

[4] J. Florik, "A Case for Considering Hyper-Rayleigh Fading Channels," *IEEE Trans. on Wireless Commun.*, vol. 6, pp. 1235–1239, Apr. 2007.

[5] A. A. Abu-Dayya and N. C. Beaulieu, "Analysis of Switched Diveristy Systems of Generalized fading Channels," *IEEE Trans. Commun.*, vol. 42, pp. 2959–2966, Nov. 1994.

[6] S. Haghani and N. C. Beaulieu, "Predetection Switched Combining in Correlated Rician Fading," *IEEE Trans. on Wireless Commun.*, vol. 6, pp. 2788–2792, Aug. 2007.

[7] C. Tellambura, A. Annamalai, and V. K. Bhargava, "Unified analysis of switched diversity systems in independent and correlated fading channels," *IEEE Trans. Commun.*, vol. 49, pp. 1955–1965, Nov. 2001.

[8] Y.-C. Ko, M.-S. Alouini, and M. K. Simon, "Analysis and optimization of switched diversity systems," *IEEE Trans. Veh. Technol.*, vol. 49, pp. 1569–1574, Sept. 2000.

[9] W. S. Lee and S. H. Oh, "Performance of Dual Switch-and-Stay Diversity NCFSK Systems over Two-Wave with Diffuse Power Fading Channels," in *6th Int. Conf. on Information, Communications and Signal Processing*, Oct. 2007, pp. 1–5.

[10] S. Haghani, "Average BER of BFSK with Postdetection Switch-and-Stay Combining in TWDP Fading," in *Proc. IEEE Vehicular Technol. Conf.*, San Francisco, CA, USA, Sept. 2011, vol. 1, pp. 1–5.

[11] J. G. Proakis, *Digital Communications*, 2nd ed. New York: McGraw-Hill, 1989.

[12] M. K. Simon and M.-S. Alouini, *Digital Communication over Fading Channels: A Unified Approach to Performance Analysis*. New York: Wiley, 2000.

[13] M. K. Simon, *Probability Distributions Involving Gaussian Random Variables: A Handbook for Engineers and Scientists*. Boston: Kluwer Academic Publishers, 2002.